Interoperability in encoded quantum repeater networks

Shota Nagayama,[1,*] Byung-Soo Choi,[2] Simon Devitt,[3] Shigeya Suzuki,[4] and Rodney Van Meter[5]
[1]*Graduate School of Media and Governance, Keio University, 5322 Endo, Fujisawa-shi, Kanagawa 252-0882, Japan*
[2]*Research Center for Quantum Information Technology, Electronics and Telecommunications Research Institute, Daejeon, South Korea*
[3]*Center for Emergent Matter Science, RIKEN, Wako, Saitama 351-0198, Japan*
[4]*Keio Research Institute at SFC, Keio University, 5322 Endo, Fujisawa-shi, Kanagawa 252-0882, Japan*
[5]*Faculty of Environment and Information Studies, Keio University, 5322 Endo, Fujisawa-shi, Kanagawa 252-0882, Japan*
(Received 2 September 2015; revised manuscript received 25 February 2016; published 26 April 2016)

The future of quantum repeater networking will require interoperability between various error-correcting codes. A few specific code conversions and even a generalized method are known, however, no detailed analysis of these techniques in the context of quantum networking has been performed. In this paper we analyze a generalized procedure to create Bell pairs encoded heterogeneously between two separate codes used often in error-corrected quantum repeater network designs. We begin with a physical Bell pair and then encode each qubit in a different error-correcting code, using entanglement purification to increase the fidelity. We investigate three separate protocols for preparing the purified encoded Bell pair. We calculate the error probability of those schemes between the Steane [[7,1,3]] code, a distance-3 surface code, and single physical qubits by Monte Carlo simulation under a standard Pauli error model and estimate the resource efficiency of the procedures. A local gate error rate of 10^{-3} allows us to create high-fidelity logical Bell pairs between any of our chosen codes. We find that a postselected model, where any detected parity flips in code stabilizers result in a restart of the protocol, performs the best.

DOI: 10.1103/PhysRevA.93.042338

I. INTRODUCTION

Much like the Internet of today, it is probable that a future quantum Internet will be a collection of radically different quantum networks utilizing some form of quantum inter-networking. These networks, called autonomous systems in the classical Internet vernacular, are deployed and administered independently and realize end-to-end communication by relaying their communication in a technology-independent distributed fashion for scalability. In the quantum regime, different error mitigation techniques may be employed within neighboring quantum networks and a type of code conversion or code teleportation between heterogeneous error-correcting codes must be provided for interoperability.

The quantum repeater is a core infrastructure component of a quantum network, tasked with constructing distributed quantum states or relaying quantum information as it routes from the source to the destination [1–4]. The quantum repeater creates new capabilities: end-to-end quantum communication, avoiding limitations on distance and the requirement for trust in quantum key distribution networks [5–7], wide-area cryptographic functions [8], distributed computation [9–15], and possibly use as physical reference frames [16–19].

Several different classes of quantum repeaters have been proposed [20–22] and these class distinctions often relate to how classical information is exchanged when either preparing a connection over multiple repeaters or sending a piece of quantum information from source to destination. The first class utilizes purification and swapping of physical Bell pairs [23–26]. First, neighboring repeaters establish raw (low-fidelity) Bell pairs that are recursively used to purify a single pair to a desired fidelity. Adjacent stations then use entanglement swapping protocols to double the total range of the entanglement. In purify and swap protocols, classical information is exchanged continuously across the entire network path to herald failures of both purification protocols and entanglement swapping. This exchange of information limits the speed of such a network significantly, especially over long distances. The second class utilizes quantum error correction (QEC) throughout the end-to-end communication [27–31] and limits the exchange of classical information to either two-way communications between adjacent repeaters or ballistic communication, where the classical information flow is unidirectional from source to receiver. These approaches either depend on high probability of success for transmitting photons over a link with high fidelity or build on the heralded creation of nearest-neighbor Bell pairs and purification, if necessary. If the probability of a successful connection between adjacent repeaters is high enough we can use quantum-error-correcting codes and relax constraints on the technology, especially memory decoherence times and the need for large numbers of qubits in individual repeaters, by sending logically encoded states hop by hop in a quasiasynchronous fashion [27,32] or using speculative or measurement-based operations [30,32,33].

Independent networks may employ any of the above schemes and within some schemes may choose different error-correcting codes or code distances. Initially deployed to support different applications and meet technological (number of qubits), logistical (availability of space), geographic (distance and topography), and economic constraints, they may use different physical implementations and will have different optimal choices for operational methods. The choice of channel types informs other design decisions. Several physical channel types have been suggested for quantum entanglement distribution over a long distance, notably, optical fiber, free space, satellite, and sneakernet [34–37]. For example, the

*kurosagi@sfc.wide.ad.jp

sneakernet approach requires such long qubit lifetimes (weeks) that QEC is necessary. It is very difficult to make a single agreement over the world in practice; in deploying the classical Internet, task forces for standardization often get tangled in politics and fail to forge a single agreement. It also often occurs that networks that are constructed individually in different locations are connected afterward. Thus, in an environment with rapidly evolving technologies, an interoperability mechanism is highly desirable and allows organizations to deploy any kind of quantum network with confidence that the network will remain useful over a long period of time.

Over time, however, it will likely become desirable to interconnect these networks into a single, larger, internetwork. In this paper we address the problem of creating end-to-end entanglement despite differences at the logical level.

These internetwork and differing operating environments can be bridged either by converting a logical qubit from one code to another or by building entanglement between two logical qubits in separate codes. Direct code conversion transforms an encoded state $|\psi\rangle_L$ into an encoded state $|\psi\rangle_{L'}$, where L and L' indicate two distinct codes. Since this change operates on valuable data, the key point is to find an appropriate fault-tolerant sequence that will convert the stabilizers from one code to the other [38–40].

Entanglement spanning two separate codes allows us to perform code teleportation. We use a heterogeneously encoded Bell pair, in which each half of the pair is encoded in a separate QEC code. Therefore, the key point is the method for preparing such a state.

Figure 1 shows an example of heterogeneously encoded Bell pairs, used at the boundary between quantum autonomous systems.[1] Quantum autonomous systems of different codes interoperate via quantum repeaters building heterogeneously encoded Bell pairs.

In this paper we give a detailed analysis of the generalized approach to create heterogeneously encoded Bell pairs for interoperability of quantum-error-correcting networks. We evaluate this approach between the Steane [[7,1,3]] code, a distance-3 surface code, and unencoded (raw) physical qubits. We chose those two codes because they have simple structure, are well investigated, and will clearly demonstrate the principle of interconnection. Figure 2 depicts a quantum repeater building and using heterogeneously encoded Bell pairs to be used in a quantum repeater.

Figure 3 depicts the quantum repeater architecture we suggest. This architecture is derived from the architecture of conventional classical routers and builds on a proposed quantum multicomputer architecture. It has several network interface cards connected to a crossbar switch, which switches interconnections among those cards for routing. This architecture is scalable since we can enlarge the crossbar and can install new network interface cards [41,42]. Therefore, quantum repeaters of this architecture can manage tens of connections,

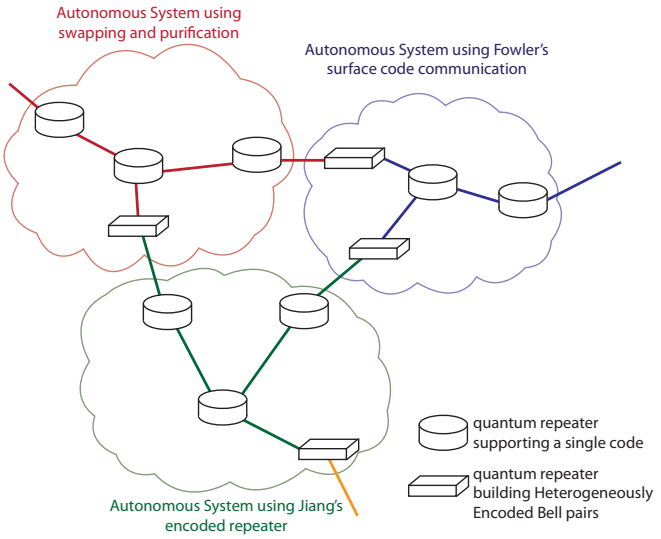

FIG. 1. Case for quantum repeaters building heterogeneously encoded Bell pairs. Each cloud represents a quantum autonomous system that is based on an error-correcting code or entanglement swapping and purification. Colored links are connections using those codes. Boxes are quantum repeaters building heterogeneously encoded Bell pairs. Cylinders are quantum repeaters, each of which supports only a single code. All links from a homogeneous repeater (cylinder) are the same type (color) since only quantum repeaters building heterogeneously encoded Bell pairs (boxes) can interoperate between different codes.

in line with the capabilities of conventional classical routers, potentially helping to advance deployment of the quantum Internet.

We have studied three possible schemes to increase the fidelity of the heterogeneously encoded Bell pairs: purification before encoding, purification after encoding, and purification after encoding with strict postselection. Purification before encoding does entanglement purification at the level of physical Bell pairs. Purification after encoding does entanglement purification at the level of encoded Bell pairs. Purification after encoding with strict postselection also does entanglement purification at the level of encoded Bell pairs. The difference from the previous scheme is that encoded Bell pairs in which any eigenvalue (error syndrome) of -1 is measured in the purification stage are discarded and the protocols restarted. (Because stabilizers are only measured during logical purification, the fourth combination of physical purification with strict postselection does not exist.) We determine the error probability and the resource efficiency of these schemes by Monte Carlo simulation with the Pauli error model of circuit level noise [43].

II. HETEROGENEOUSLY ENCODED BELL PAIRS

There are two methods for building heterogeneously encoded Bell pairs for code teleportation. The first is to inject each qubit of a physical Bell pair into a different code [44]. The second is to prepare a common Schrödinger cat state for two codes to check the ZZ parity of two logical qubits [45–47]. It has been shown that code teleportation utilizing a Schrödinger

[1]In the classical Internet, significant differences may occur even between subnets of a single AS, but for simplicity in this paper we will restrict ourselves to the assumption that a quantum AS is internally homogeneous.

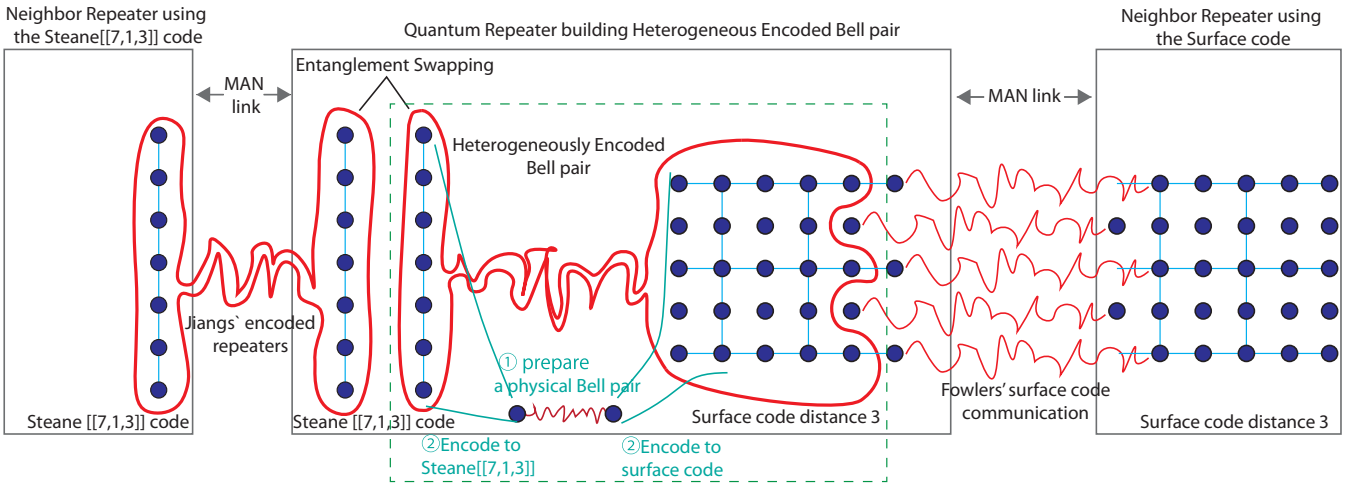

FIG. 2. Heterogeneously encoded Bell pairs can be used to bridge quantum networks using different error-correcting mechanisms. MAN stands for the metropolitan area network. A blue circle denotes a physical qubit. A set of blue lines indicates qubits that comprise an encoded qubit. Each thin red line describes an entanglement between physical qubits. Each thick red loop outlines entanglement between encoded qubits. The half of the Bell pair encoded in the surface code can be sent to the neighboring quantum repeater by the method of Fowler *et al.* [29]. The other half of the Bell pair, encoded in the Steane [[7,1,3]] code, undergoes entanglement swapping with a Steane [[7,1,3]]—Steane [[7,1,3]] encoded Bell pair established via the method of Jiang *et al.* [28]. Therefore, this central quantum repeater can create entanglement between the two quantum repeaters in different types of networks. In the green dashed rectangle is the procedure for encoding a Bell pair heterogeneously. A qubit of a Bell pair is encoded in the Steane [[7,1,3]] code on the left side of the figure, adding six qubits. The other qubit of the Bell pair is encoded onto the surface code of distance 3, adding 24 qubits on the right side of the figure. Multiple copies are prepared, entangled, and purified. Eventually, a heterogeneously encoded logical Bell pair is achieved with high enough fidelity to enable coupling of the two networks. Ancilla qubits for syndrome measurement are depicted in the surface code, while those are not depicted in the Steane code.

cat state is better than direct code conversion because the necessary stabilizer checking for the latter approach is too expensive [48]. Direct code conversion and code teleportation utilizing a Schrödinger cat state are specific for a chosen code pair as the specific sequence of fault-tolerant operations has to match the two codes chosen. In contrast, code teleportation by injecting a physical Bell pair can be used for any two codes and provided encoding circuits are available for the two codes in question, the protocol can be generalized to arbitrary codes.

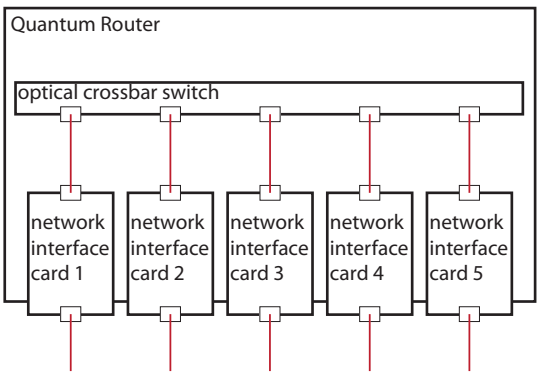

FIG. 3. Architecture of a scalable quantum repeater supporting routing. Each red line describes a photonic connection. The crossbar switch switches interconnections of network interface cards (NICs). Each network interface card is connected to another quantum repeater or computer at the open ends of the red lines. By using a crossbar switch, interconnections do not interrupt each other, so this architecture is scalable. The dashed green box in Fig. 2 corresponds to creating heterogeneous Bell pairs between, e.g., NIC1 and NIC2. Step 1 in Fig. 2 is the creation of physical Bell pairs via the optical crossbar switch. Step 2 takes place via local gates within the respective NICs.

Putting things together, heterogeneous Bell pairs of long distance can be created by entanglement swapping (physical or logical) or a method appropriate to each network, allowing an arbitrary quantum state encoded in some code to be moved onto another code by teleportation [28,29]. In a single computer, code conversion has been proposed for memory hierarchies and for cost-effective fault-tolerant quantum computation [38,44,46,49–51].

The green dashed rectangle in Fig. 2 shows the basic procedure for creating a heterogeneously encoded logical Bell pair. Each circle denotes a physical qubit and thin blue lines connecting those circles demarcate the set of physical qubits comprising a logical qubit. Each qubit of a Bell pair is processed separately and encoded onto its respective code through non-fault-tolerant methods to create arbitrary encoded states.

Figure 4 shows the circuit to encode an arbitrary quantum state in the Steane [[7,1,3]] code [52–54]. Figure 5 shows the circuit to encode an arbitrary quantum state in the surface code [55].

The KQ of a circuit is the number of qubits times the circuit depth, giving an estimate of the number of opportunities for errors to occur [52]. Note that those circuits are not required to be fault tolerant because the state being purified is generic, rather than irreplaceable data. If the fidelity of the encoded Bell pair is not good enough (e.g., as determined operationally using quantum state tomography), entanglement purification is performed [56,57].

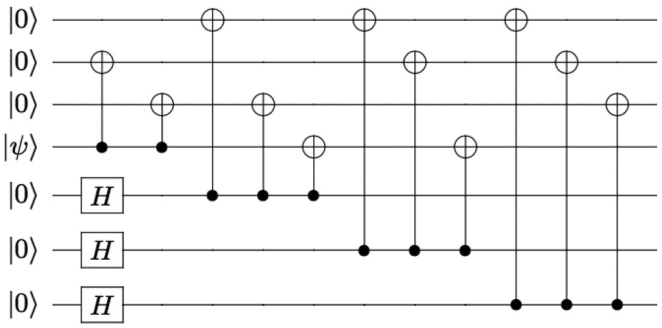

FIG. 4. Circuit to encode an arbitrary state to the Steane [[7,1,3]] code. Here $|\psi\rangle$ is the state to be encoded. This circuit is not fault tolerant. The KQ of this circuit is 42 because some gates can be performed simultaneously.

III. THREE METHODS TO PREPARE A HETEROGENEOUSLY ENCODED HIGH-FIDELITY BELL PAIR

Entanglement purification is performed to establish high-fidelity entanglement [58,59]. Entanglement purification can be viewed as a distributed procedure for testing a proposition about a distributed state [21].

Figure 6 shows the circuit for the basic form of entanglement purification where $|\phi\rangle$ is a noisy Bell pair. The input is two low-fidelity Bell pairs and on success the output is a Bell pair of higher fidelity. One round of purification suppresses one type of error, X or Z. If the initial Bell pairs are Werner states, or approximately Werner states, then to suppress both types, two rounds of purification are required. The first round transforms the resulting state into a binary state with only one significant error term but not a significantly improved fidelity.

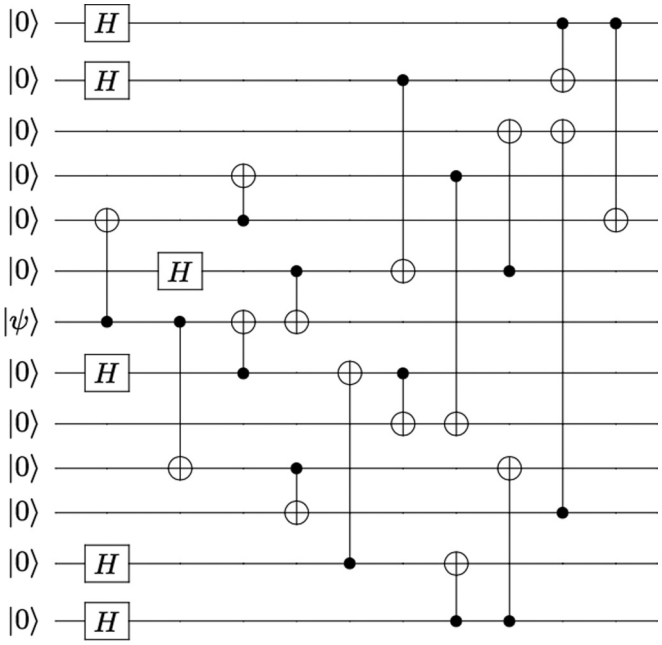

FIG. 5. Circuit to encode an arbitrary state $|\psi\rangle$ to a distance-3 surface code [55]. This circuit is not fault tolerant. The KQ of this circuit is 250 if some gates are performed simultaneously.

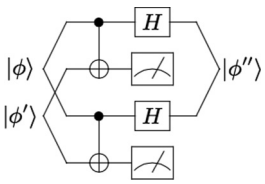

FIG. 6. Circuit for entanglement purification [2]. The two measured values are compared. If they disagree, the output qubits are discarded. If they agree, the output qubits are treated as a new Bell pair. At this point, the X error rate of the output Bell pair is suppressed from the input Bell pairs. The Hadamard gates exchange the X and Z axes, so the following round of purification suppresses the Z error rate. As a result, entanglement purification consumes two Bell pairs and generates a Bell pair of higher fidelity stochastically.

The second round then strongly suppresses errors if the gate error rate is small. Thus, the overall fidelity tends to improve in a stair step fashion. After two rounds of purification, the distilled fidelity will be, in the absence of local gate error,

$$F'' \sim \frac{F^2}{F^2 + (1-F)^2}, \tag{1}$$

where the original state is the Werner state

$$\rho = F|\Phi^+\rangle\langle\Phi^+| + \frac{1-F}{3}(|\Phi^-\rangle\langle\Phi^-| + |\Psi^+\rangle\langle\Psi^+| + |\Psi^-\rangle\langle\Psi^-|) \tag{2}$$

and F is the fidelity $F = \langle\phi|\rho|\phi\rangle$ if $|\phi\rangle$ is the desired state. The probability of success of a round of purification is

$$p = F^2 + 2F\frac{1-F}{3} + 5\left(\frac{1-F}{3}\right)^2. \tag{3}$$

Table I in Appendix A provides the numerical data for this to compare with our protocols. Our simulation assumptions are detailed in Sec. IV.

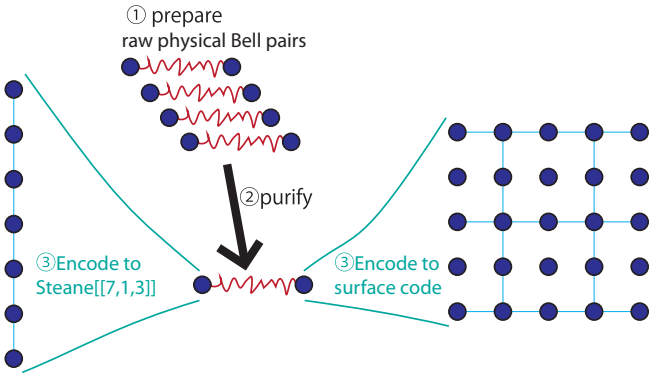

FIG. 7. Overview of the scheme that purifies physical Bell pairs to generate an encoded Bell pair of high fidelity. First, entanglement purification is conducted between physical Bell pairs an arbitrary number of times. Second, each qubit of the purified physical Bell pair is encoded to a heterogeneous error-correcting code.

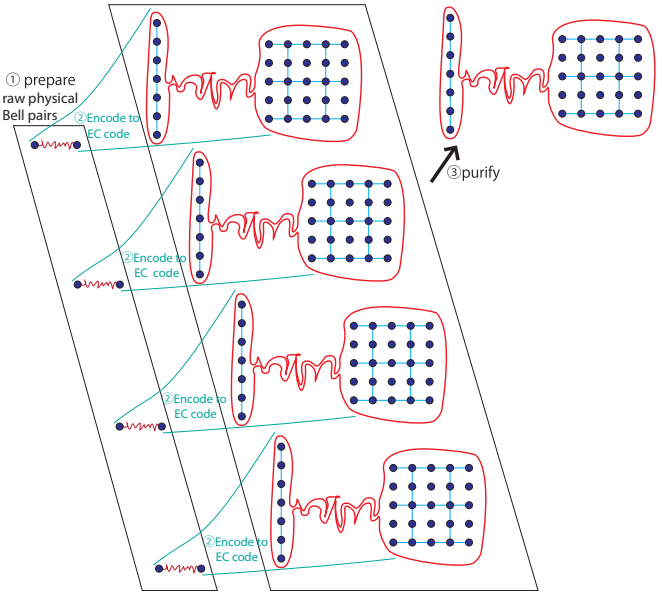

FIG. 8. Overview of the scheme that purifies encoded Bell pairs to achieve an encoded Bell pair of high fidelity. In this method, first, raw physical Bell pairs are encoded into our heterogeneous error-correcting code, Second, those heterogeneously encoded Bell pairs are purified directly at the logical level.

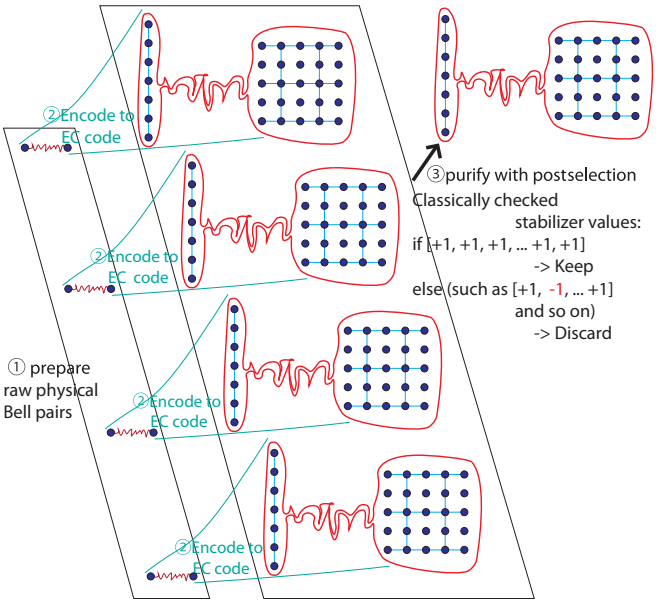

FIG. 9. Overview of the scheme that purifies encoded Bell pairs to achieve an encoded Bell pair of high fidelity with strict postselection. First, raw physical Bell pairs are encoded to a heterogeneous error-correcting code, the same as purification after encoding. Second, at measurement in purification, eigenvalues of each stabilizer are checked classically. If any eigenvalue of -1 is measured, the output Bell pair is discarded (in a manner similar to if the overlying purification protocol failed).

A. Purification before encoding

Figure 7 shows the overview of the scheme to make heterogeneously encoded Bell pairs that are purified before encoding. To create an encoded Bell pair of high fidelity, entanglement purification is repeated the desired number of times. Next, each qubit of the purified Bell pair is encoded to its respective error-correcting code. To estimate the rate of logical error after encoding, we perform a perfect syndrome extraction of the system to remove any residual correctable errors. After the whole procedure finishes, we check whether logical errors exist. Table II in Appendix A presents the details of the simulated error probability and resource efficiency of purification before encoding.

B. Purification after encoding

Figure 8 shows the overview of the scheme to make heterogeneously encoded Bell pairs that are purified after encoding. In this scheme, to create an encoded Bell pair of high fidelity, heterogeneously encoded Bell pairs are generated first by encoding each qubit of a raw physical Bell pair to our chosen heterogeneous error-correcting codes. Next, those encoded Bell pairs are purified at the logical level the desired number of times, via transversal CNOT gates and logical measurements. Logical purification is also achieved by the circuit shown in Fig. 6, operating on logical rather than physical qubits. Table III presents the details of the simulated error probability and resource efficiency of purification after encoding.

C. Purification after encoding with strict postselection

Figure 9 shows the overview of the scheme to make encoded Bell pairs, purified after encoding with strict postselection protocols to detect errors. This scheme uses a procedure similar to purification after encoding. In this scheme, to create an encoded Bell pair of high fidelity, heterogeneously encoded Bell pairs are generated first by encoding each qubit of a raw physical Bell pair to our chosen heterogeneous error-correcting codes. We then run purification protocols at the logical level, similarly to the previous protocol. However, when we perform a logical measurement as part of this protocol, we also calculate (classically) the eigenvalues of all code stabilizers. If any of these eigenvalues are found to be negative, we treat the operation as a failure (in a manner similar to odd-parity logical measurements for the purification) and the output Bell pair of the purification is discarded. This simultaneously performs purification and error correction using the properties of the codes. Table IV presents the details of the numerically calculated error probability and resource efficiency of purification after encoding with strict postselection.

IV. ERROR SIMULATION AND RESOURCE ANALYSIS

We calculate the error probability and estimate resource requirements by Monte Carlo simulation. The physical Bell pairs' fidelity is assumed to be 0.85; the state is assumed to be, following Nölleke *et al.* [60],

$$\rho = 0.85|\Phi^+\rangle\langle\Phi^+| + 0.04|\Phi^-\rangle\langle\Phi^-| + 0.055|\Psi^+\rangle\langle\Psi^+| + 0.055|\Psi^-\rangle\langle\Psi^-|. \quad (4)$$

We have chosen to model our interface-to-interface coupling as an optical coupling, based on the experimental values of Nölleke *et al.* [60]. This organization corresponds to a classical

Internet router architecture in which separate network interface cards connect to each other through a crossbar switch on a backplane as shown in Fig. 3, which in our case is assumed to be an intermediate-fidelity optical connection [61]. Although the exact numerical results will of course vary, the principles described in this paper are independent of the exact numbers. For comparison, Tables VII–IX in Appendix B present results of simulations in which raw Bell pairs are created using local gates, an approach that could be used with a simpler but less scalable repeater architecture.

Our error model is the Pauli model of circuit level noise [43]. This model consists of memory error, one-qubit gate error, two-qubit gate error, and measurement error, each of which occurs with the error probability p. Memory, one-qubit gates, and measurement are all vulnerable to X, Y, and Z errors and we assume a balanced model, where probabilities are $\frac{p}{3}$ respectively. Similarly, two-qubit gates are vulnerable to all 15 possibilities, each with a probability of $\frac{p}{15}$. Errors propagate during all circuits after the initial distribution of Bell pairs.

Figure 10 shows a baseline homogeneous simulation creating logical Bell pairs of Steane [[7,1,3]] code using our physical-to-logical mechanism. The figure plots the number of consumed raw physical Bell pairs versus logical error rate in the output state. Figure 11 shows a similar baseline homogeneous simulation for a surface code of distance 3. The difference between purification before encoding and purification of physical Bell pairs indicates how many logical errors are introduced during the encoding process. Purification after encoding may show that the surface code of distance 3 is more suitable than the Steane [[7,1,3]], however, because those local gate error rates are greater than the threshold of the Steane [[7,1,3]] code it is hard to judge fairly.

Figure 12 plots the number of consumed raw physical Bell pairs versus logical error rate in the output state for the heterogeneous Steane [[7,1,3]]–surface code distance-3 case. This heterogeneous result falls near the average of those two baseline homogeneous simulations above. The $\max\left|\frac{\text{heterogeneous result}}{\text{average of homogeneous result}} - 1\right|$ is 0.086. The $\text{av}\left|\frac{\text{heterogeneous result}}{\text{average of homogeneous result}}\right|$ is 1.007. Since the depth of the circuit of the heterogeneous simulation is aligned to the longer depth of the two codes, the heterogeneous result is a bit higher than the average of the homogeneous simulations.

The numbers of raw Bell pairs consumed declines as the local gate error rate is lowered. This is because the influence of the local gate error rate shrinks relative to the infidelity of generated raw Bell pairs. If the system is free from local gate error, the numbers of raw Bell pairs consumed by the three

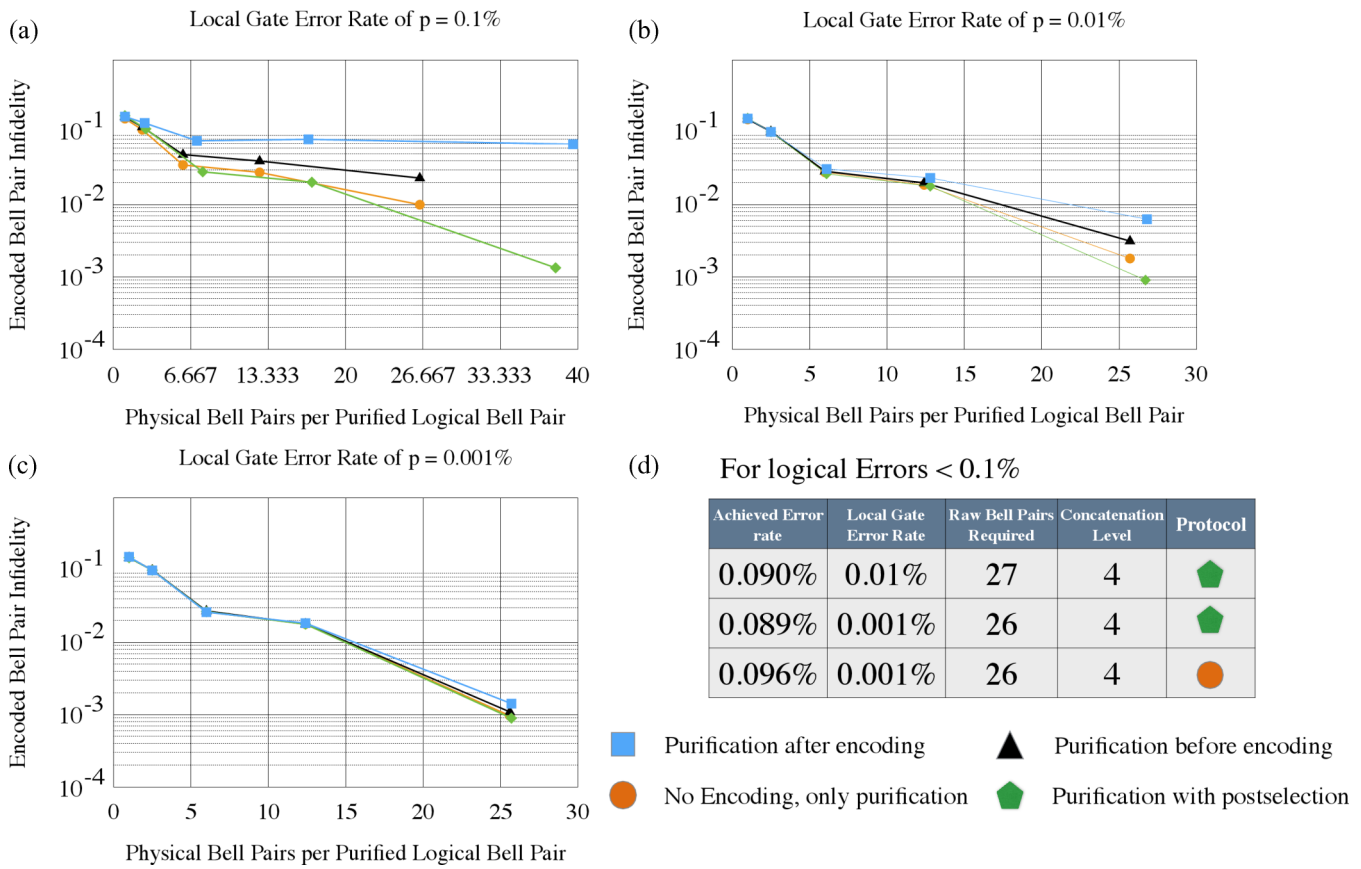

Achieved Error rate	Local Gate Error Rate	Raw Bell Pairs Required	Concatenation Level	Protocol
0.090%	0.01%	27	4	⬟
0.089%	0.001%	26	4	⬟
0.096%	0.001%	26	4	●

FIG. 10. Results of a baseline simulation of creation of a Steane [[7,1,3]]–Steane [[7,1,3]] homogeneous Bell pair, showing residual logical error rate versus physical Bell pairs consumed. The three schemes plus the baseline case of purification of physical Bell pairs are each represented by a line. Each point along a line corresponds to the number of rounds of purification. The leftmost point represents no purification, the second point is one round of purification, and the rightmost point represents four rounds of purification (a)–(c). Improving values of local gate error rate. (d) The three cases with residual error rate of 10^{-3} or less.

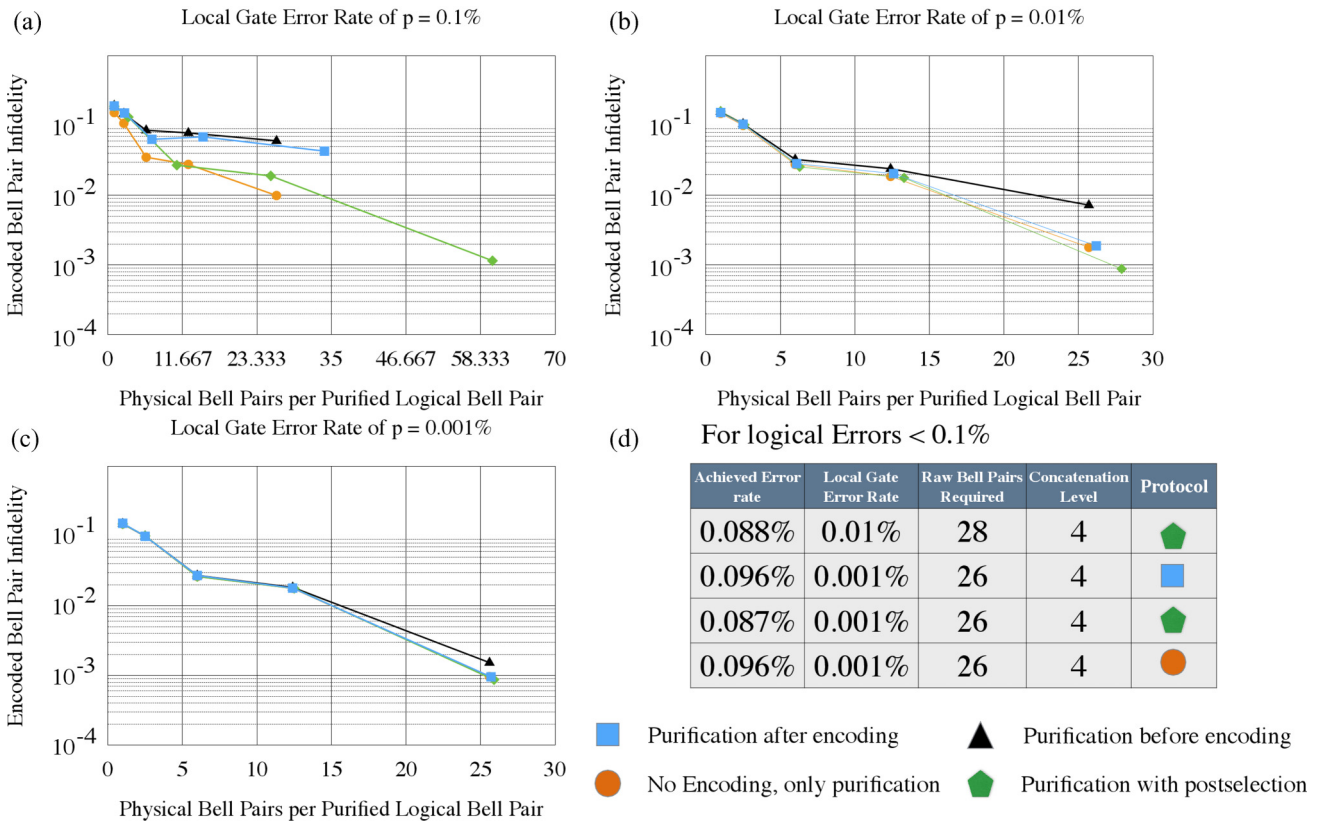

Achieved Error rate	Local Gate Error Rate	Raw Bell Pairs Required	Concatenation Level	Protocol
0.088%	0.01%	28	4	
0.096%	0.001%	26	4	
0.087%	0.001%	26	4	
0.096%	0.001%	26	4	

FIG. 11. Results of a baseline simulation of creation of a surface code distance-3–surface code distance-3 homogeneous Bell pair, showing the residual logical error rate versus physical Bell pairs consumed. Other conditions and definitions are as in Fig. 10.

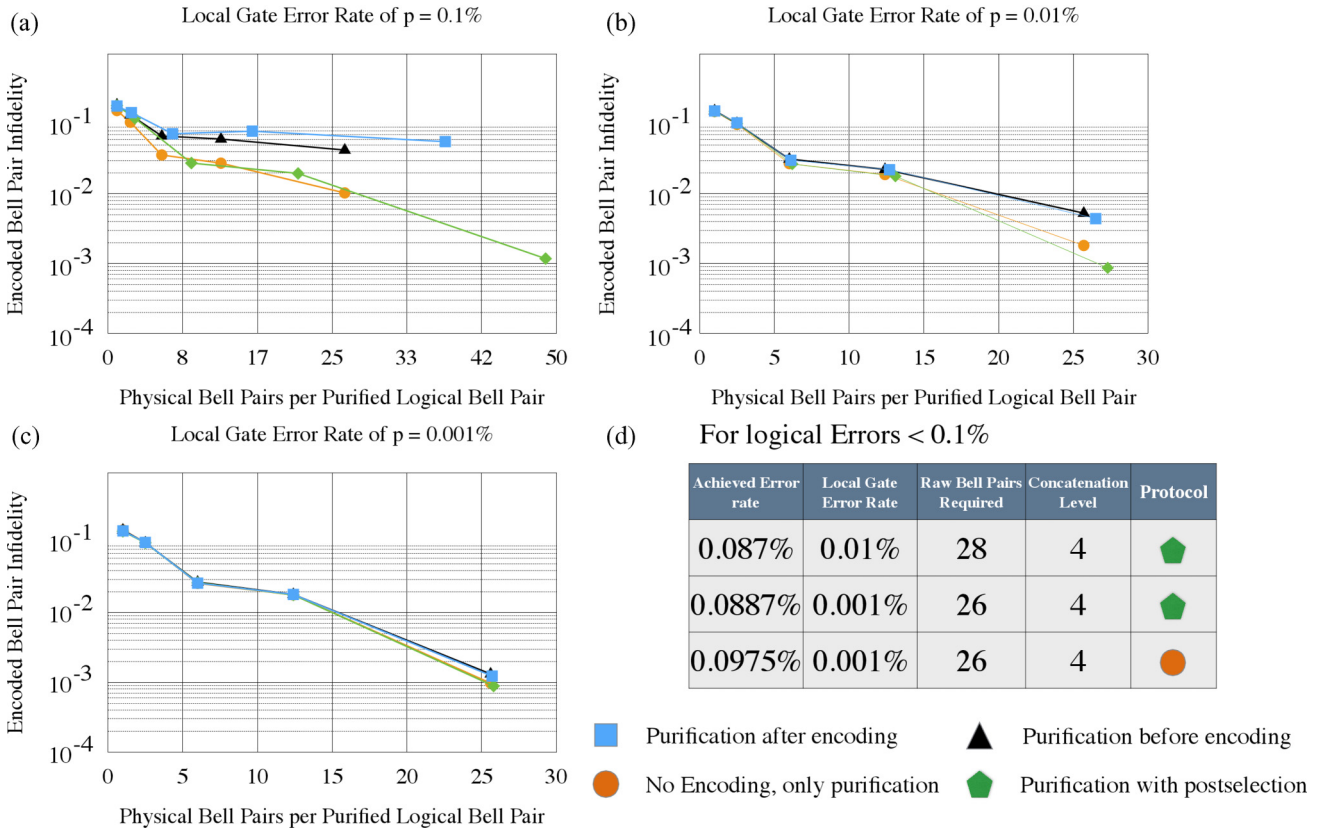

Achieved Error rate	Local Gate Error Rate	Raw Bell Pairs Required	Concatenation Level	Protocol
0.087%	0.01%	28	4	
0.0887%	0.001%	26	4	
0.0975%	0.001%	26	4	

FIG. 12. Results of simulation of creation of a Steane [[7,1,3]]–surface code distance-3 heterogeneous Bell pair, showing residual logical error rate versus physical Bell pairs consumed. Other conditions and definitions are as in Fig. 10.

schemes must converge. At $p = 10^{-5}$, the required numbers of raw Bell pairs of the schemes are essentially identical and they require about 26 raw Bell pairs to achieve four rounds of purification. Higher efficiency would require improving the initial fidelity of $F = 0.85$.

At any error rate and with any number of rounds of purification from 0 to 4, purification before encoding and purification after encoding result in fidelity worse than simple purification of physical Bell pairs. This suggests that errors accumulated during encoding are difficult to correct. On the other hand, purification after encoding with strict postselection gives better results than simple purification, at the expense of consuming more raw physical Bell pairs. This difference is noticeable at $p = 10^{-3}$; 49 raw physical Bell pairs are used to create an encoded Bell pair purified four rounds. The local gate error rate is so high that an eigenvalue of -1 is often found at the measurement in purification and the output Bell pair is discarded. For purification after encoding with postselection, the residual error rate after n rounds of purification is similar at any p, but resource demands change. It converts local errors into loss, or discarded states. Therefore, purification after encoding with postselection is dominated by the original raw Bell pair infidelity. At $p = 10^{-3}$, purification after encoding also requires more raw physical Bell pairs than the other schemes, because the error rate after purification is so high that the success probability of purification is poor.

Though more rounds of purification are supposed to result in smaller logical error rate, three rounds of purification of purification after encoding at $p = 10^{-3}$ give an error rate *larger* than that of two rounds. The local gate error rate is too high and purification introduces more errors than it suppresses on odd-numbered purification rounds.

Purification after encoding with strict postselection gives similar results for the two local gate error rates $p = 10^{-4}$ and 10^{-5}. The difference is a small number of consumed raw physical Bell pairs. Even at $p = 10^{-3}$, we see that four rounds of purification drives the residual error rate down almost to 0.1%. From this fact we conclude that $p = 10^{-3}$ will be a good enough local gate error rate to allow us to create heterogeneously encoded Bell pairs, suitable for many purposes, from raw physical Bell pairs of $F = 0.85$.

V. DISCUSSION

We have proposed and analyzed a generalized method for creating heterogeneously encoded Bell pairs that can be used for interoperability between encoded networks. This is the first step in examining the full design of interconnection routers for quantum repeater systems utilizing different error mitigation techniques. Our results have shown that purification after encoding with strict postselection is a better preparation method than our other two candidates. Strict postselection of two rounds of purification results in better fidelity than error correction of four rounds of purification at all error rates and better physical Bell pair efficiency. Since the threshold of the error rate of the Steane [[7,1,3]] code is around 10^{-4}, our simulations of purification before encoding and purification after encoding of $\sim 10^{-4}$ do not show an advantage compared to simple physical purification; however, strict postselection does. Purification after encoding with strict postselection has a higher threshold than the normal encoding and purification have. With an initial $F = 0.85$, we can almost reach a residual error rate of 10^{-3} using four rounds of purification, for physical Bell pairs at $p = 10^{-5}$ or postselected heterogeneous pairs at $p = 10^{-4}$. The Bell pairs built here exist inside a single quantum router and are used as a single element in building end-to-end quantum entanglement spanning multiple hops as in Fig. 1. Thus, the end-to-end fidelity depends on many factors outside this box.

As we noted in the Introduction, quantum repeater networks will serve several purposes, potentially requiring different residual error levels on the end-to-end quantum communication. Networks using physical purify-and-swap technologies, for example, will easily support quantum key distribution, but distributed numeric computation will require building error correction on top of the Bell pairs provided by the network. Our simulations of heterogeneous Bell pairs where one half is a physical qubit, rather than logically encoded, are described in Appendix B. These simulations show that residual error rates can be suppressed successfully, allowing us to bridge these separate types of networks and support the deployment of any application suitable for purify-and-swap networks across a heterogeneous quantum Internet. The error rates we have achieved for each heterogeneous technology pair demonstrate the effectiveness of our heterogeneous scheme for interoperability. Moreover, operation appears to be feasible at a local gate error rate of 10^{-3} and at 10^{-4} operation is almost indistinguishable from having perfect local gates.

Quantum error correction generally corrects up to $e \leqslant \lfloor \frac{d-1}{2} \rfloor$ errors per block and detects but miscorrects $\frac{d-1}{2} < e < d$ errors. Postselection eliminates this miscorrection possibility, leaving only groups of d errors or errors that occur after syndrome extraction in the state. The structure of Calderbank, Shor and Steane (CSS) codes is so self-similar that we expect that the analysis will be useful for evaluating other hardware models and CSS codes.

The analysis presented here is useful not only in the abstract, but also serves as a first step toward a hardware design for a multiprotocol quantum router (the boxes in Fig. 1). Such a router may be built on a quantum multicomputer architecture, with several small quantum computers coupled internally via a local optical network [61–64]. This allows hardware architects to build separate small devices to connect to each type of network and then to create Bell pairs between these devices using the method described in this paper. In addition, this method can be used within large-scale quantum computers that wish to use different quantum-error-correcting codes for different purposes, such as long-term memory or ancilla state preparation.

This scheme is internal to a single repeater at the border of two networks and will allow effective end-to-end communication where errors across links are more important than errors within a repeater node. It therefore can serve as a building block for a quantum Internet.

ACKNOWLEDGMENTS

This work was supported by JSPS KAKENHI Grants No. 25280034 and No. 25:4103. We thank Joe Touch for valuable technical conversations.

TABLE I. Our baseline case, discrete simulation using physical entanglement purification only. The merged error rate is the probability that either X error or Z error occurs. The physical Bell pair inefficiency is (No. of created raw Bell pairs)/(No. of purified Bell pairs). KQ is (No. of qubits) × (No. of steps). In this simulation, KQ is the number of chances that errors may occur.

No. of purifications	X error rate	Z error rate	Merged error rate	Physical Bell pair inefficiency	KQ	No. of single-qubit gates	No. of two-qubit gates
			(a) Local gate error rate of 10^{-3}				
0	0.113	0.1	0.156	1.0	88	86	1
1	0.096	0.0197	0.106	2.5	98	91	5
2	0.0247	0.0154	0.036	6.0	122	103	14
3	0.0248	0.00498	0.0275	12.6	167	125	32
4	0.00753	0.00523	0.0103	26.4	262	173	70
			(b) Local gate error rate of 10^{-4}				
0	0.109	0.0968	0.151	1.0	88	86	1
1	0.0915	0.0151	0.0988	2.5	98	91	5
2	0.0183	0.0104	0.0271	6.0	122	103	14
3	0.0183	0.000796	0.0189	12.4	166	125	32
4	0.00125	0.000796	0.00182	25.7	258	171	68
			(c) Local gate error rate of 10^{-5}				
0	0.112	0.0963	0.152	1.0	88	86	1
1	0.0928	0.0152	0.101	2.5	98	91	5
2	0.0177	0.0102	0.0262	6.0	121	103	14
3	0.0176	0.000381	0.0179	12.4	166	125	32
4	0.000633	0.000371	0.000975	25.6	257	171	68

APPENDIX A: SIMULATION DATA FOR $F = 0.85$ RAW BELL PAIRS ON MULTIPLE-NIC ROUTER ARCHITECTURE

Table I shows our baseline simulation results using physical entanglement only with no encoding. Table II shows the simulated results of purification before encoding for a Bell pair of a single layer of the Steane [[7,1,3]] code and a distance-3 surface code. Table III shows the simulated results of the scheme purification after encoding of the same codes. Table IV shows the simulated results of the scheme

TABLE II. Simulation results of purification before encoding for a Bell pair of a single layer of the Steane [[7,1,3]] code and a distance-3 surface code. Other conditions and definitions are as in Table I.

No. of purifications	X error rate	Z error rate	Merged error rate	Physical Bell pair inefficiency	KQ	No. of single-qubit gates	No. of two-qubit gates
			(a) Local gate error rate of 10^{-3}				
0	0.128	0.12	0.188	1.0	5402	4130	636
1	0.111	0.0379	0.135	2.5	5412	4135	640
2	0.0402	0.0355	0.0674	6.0	5436	4147	649
3	0.0421	0.0258	0.061	12.6	5481	4170	667
4	0.0231	0.0251	0.0424	26.4	5576	4217	705
			(b) Local gate error rate of 10^{-4}				
0	0.114	0.0976	0.155	1.0	5402	4130	636
1	0.0927	0.0173	0.102	2.5	5412	4135	640
2	0.02	0.0136	0.0315	6.0	5436	4147	649
3	0.0201	0.00293	0.0224	12.4	5480	4169	667
4	0.00298	0.0029	0.00529	25.7	5572	4215	703
			(c) Local gate error rate of 10^{-5}				
0	0.11	0.0953	0.152	1.0	5402	4130	636
1	0.0922	0.015	0.0999	2.5	5412	4135	640
2	0.0183	0.0106	0.0273	6.0	5436	4147	649
3	0.0177	0.000598	0.0182	12.4	5480	4169	667
4	0.000797	0.000583	0.00132	25.6	5571	4215	703

TABLE III. Simulation results of the scheme purification after encoding between the Steane [[7,1,3]] code and the distance-3 surface code. Other conditions and definitions are as in Table I.

No. of purifications	X error rate	Z error rate	Merged error rate	Physical Bell pair inefficiency	KQ	No. of single-qubit gates	No. of two-qubit gates
			(a) Local gate error rate of 10^{-3}				
0	0.126	0.115	0.181	1.0	5402	4130	636
1	0.131	0.0311	0.146	2.6	6892	5477	722
2	0.0412	0.039	0.0726	7.2	10967	9159	956
3	0.0693	0.0137	0.079	16.1	19068	16480	1425
4	0.0278	0.031	0.0559	37.6	38536	34071	2550
			(b) Local gate error rate of 10^{-4}				
0	0.11	0.0983	0.154	1.0	5402	4130	636
1	0.0958	0.0159	0.104	2.5	6776	5370	716
2	0.0198	0.0125	0.0303	6.1	10061	8335	907
3	0.0213	0.0012	0.0222	12.7	16134	13814	1262
4	0.00222	0.00237	0.00442	26.5	28864	25300	2005
			(c) Local gate error rate of 10^{-5}				
0	0.108	0.0957	0.148	1.0	5402	4130	636
1	0.0931	0.015	0.101	2.5	6759	5355	715
2	0.018	0.01	0.0264	6.0	9961	8244	901
3	0.0178	0.000395	0.0182	12.4	15880	13584	1247
4	0.000729	0.000515	0.00123	25.7	28149	24652	1965

purification after encoding with strict postselection. Since purification at the level of encoded qubits consists of logical gates, purification before encoding has a much smaller KQ than the other two schemes. Purification after encoding with strict postselection discards more qubits than purification after encoding does to create a purified encoded Bell pair, so purification after encoding with strict postselection also results in a larger KQ. Table V shows the simulated results of the scheme purification after encoding with strict postselection between the Steane [[7,1,3]] code and the nonencoded physical half. Table VI shows the simulated results of the scheme purification after encoding with strict postselection between the distance-3 surface code and the nonencoded physical half.

TABLE IV. Simulation results of the scheme purification after encoding with strict postselection between the Steane [[7,1,3]] code and the distance-3 surface code. Other conditions and definitions are as in Table I. The values at $p = 10^{-4}$ and 10^{-5} demonstrate that the residual error rate saturates after more than one round of purification.

No. of purifications	X error rate	Z error rate	Merged error rate	Physical Bell pair inefficiency	KQ	No. of single-qubit gates	No. of two-qubit gates
			(a) Local gate error rate of 10^{-3}				
0	0.13	0.118	0.184	1.0	5402	4130	636
1	0.114	0.0146	0.121	3.0	7173	5732	737
2	0.018	0.0113	0.0276	9.3	12748	10774	1053
3	0.0193	0.000387	0.0196	21.2	23398	20403	1661
4	0.000776	0.000414	0.00118	48.8	47963	42611	3063
			(b) Local gate error rate of 10^{-4}				
0	0.108	0.0981	0.152	1.0	5402	4130	636
1	0.0948	0.0149	0.102	2.5	6797	5389	717
2	0.0177	0.0104	0.0267	6.2	10173	8437	913
3	0.0176	0.000343	0.0179	13.1	16442	14094	1278
4	0.000545	0.000326	0.00087	27.3	29540	25912	2042
			(c) Local gate error rate of 10^{-5}				
0	0.109	0.0917	0.146	1.0	5402	4130	636
1	0.0921	0.0153	0.0996	2.5	6766	5361	715
2	0.0181	0.0101	0.0268	6.0	9968	8251	902
3	0.0176	0.000333	0.0179	12.4	15913	13614	1249
4	0.000572	0.000317	0.000887	25.8	28213	24710	1968

TABLE V. Simulation results of the scheme purification after encoding with strict postselection between the Steane [[7,1,3]] code and the nonencoded physical half. Other conditions and definitions are as in Table I.

No. of purifications	X error rate	Z error rate	Merged error rate	Physical Bell pair inefficiency	KQ	No. of single-qubit gates	No. of two-qubit gates
			(a) Local gate error rate of 10^{-3}				
0	0.116	0.107	0.166	1.0	4260	3660	300
1	0.103	0.0171	0.111	2.6	5367	4709	330
2	0.022	0.013	0.0325	6.9	8234	7425	409
3	0.0227	0.00142	0.0236	15.0	13692	12595	559
4	0.0028	0.00155	0.00386	32.5	25548	23825	884
			(b) Local gate error rate of 10^{-4}				
0	0.11	0.0951	0.151	1.0	4260	3660	300
1	0.0948	0.0154	0.103	2.5	5281	4627	328
2	0.0179	0.0103	0.0266	6.1	7713	6929	395
3	0.0181	0.000438	0.0184	12.6	12201	11179	518
4	0.00077	0.000429	0.00115	26.2	21554	20033	775
			(c) Local gate error rate of 10^{-5}				
0	0.11	0.097	0.152	1.0	4260	3660	300
1	0.0929	0.0155	0.101	2.5	5274	4620	328
2	0.0182	0.0101	0.0267	6.0	7659	6878	393
3	0.0176	0.00035	0.0179	12.4	12069	11053	515
4	0.000577	0.000334	0.000904	25.7	21200	19697	766

APPENDIX B: SIMULATION DATA FOR BELL PAIR CREATION VIA LOCAL GATES

Data in this Appendix are from simulations in which raw Bell pairs are created by local gates, two initializations, a Hadamard gate, an identity gate, and a CNOT gate. Table VII shows the simulated results using physical entanglement only with no encoding. Table VIII shows the simulated results of the scheme purification after encoding for a Bell pair of a single layer of the Steane [[7,1,3]] code and a distance-3 surface code. Table IX shows the simulated results of the scheme purification after encoding with strict postselection for a Bell pair of a single layer of the Steane [[7,1,3]] code and a distance-3 surface code.

The fidelity of raw Bell pairs created via local gates is much better than 0.85, lowering the need for purification.

TABLE VI. Simulation results of the scheme purification after encoding with strict postselection between the distance-3 surface code and the nonencoded physical half. Other conditions and definitions are as in Table I.

No. of purifications	X error rate	Z error rate	Merged error rate	Physical Bell pair inefficiency	KQ	No. of single-qubit gates	No. of two-qubit gates
			(a) Local gate error rate of 10^{-3}				
0	0.13	0.113	0.181	1.0	1188	914	137
1	0.116	0.0172	0.125	2.8	1985	1611	202
2	0.0224	0.0135	0.0334	8.2	4321	3652	393
3	0.0227	0.00145	0.0236	18.3	8739	7511	755
4	0.0028	0.00154	0.00386	40.9	18625	16148	1566
			(b) Local gate error rate of 10^{-4}				
0	0.114	0.0959	0.154	1.0	1188	914	137
1	0.0943	0.0157	0.102	2.5	1864	1504	193
2	0.0179	0.0105	0.0267	6.2	3481	2915	328
3	0.018	0.000445	0.0184	12.9	6482	5533	580
4	0.000808	0.000438	0.0012	26.9	12728	10982	1104
			(c) Local gate error rate of 10^{-5}				
0	0.108	0.0934	0.147	1.0	1188	914	137
1	0.091	0.0152	0.0988	2.5	1848	1490	192
2	0.0179	0.0105	0.0267	6.0	3410	2853	323
3	0.0176	0.000336	0.0179	12.4	6294	5368	565
4	0.000589	0.00033	0.000911	25.8	12266	10578	1067

TABLE VII. Results of simulation in which raw Bell pairs are created using local gates and using physical entanglement purification only. Other conditions and definitions are as in Table I.

No. of purifications	X error rate	Z error rate	Merged error rate	Physical Bell pair inefficiency	KQ	No. of single-qubit gates	No. of two-qubit gates
			(a) Local gate error rate of 10^{-3}				
0	0.00444	0.00447	0.00736	1.0	88	90	1
1	0.00777	0.0047	0.0101	2.0	96	98	4
2	0.00629	0.00452	0.00858	4.1	112	115	10
			(b) Local gate error rate of 10^{-4}				
0	0.000445	0.00045	0.000731	1.0	88	90	1
1	0.000768	0.000456	0.000995	2.0	96	98	4
2	0.000644	0.000468	0.000875	4.0	112	114	10
			(c) Local gate error rate of 10^{-5}				
0	0.0000446	0.0000464	0.000075	1.0	88	90	1
1	0.0000779	0.0000457	0.000101	2.0	96	98	4
2	0.0000635	0.0000438	0.0000851	4.0	112	114	10

TABLE VIII. Simulation results of purification after encoding for a Bell pair of a single layer of the Steane [[7,1,3]] code and a distance-3 surface code. Raw Bell pairs are created using local gates. Other conditions and definitions are as in Table I.

No. of purifications	X error rate	Z error rate	Merged error rate	Physical Bell pair inefficiency	KQ	No. of single-qubit gates	No. of two-qubit gates
			(a) Local gate error rate of 10^{-3}				
0	0.0221	0.0255	0.0419	1.0	5402	4134	636
1	0.0371	0.00451	0.0399	2.2	6521	5148	702
2	0.00697	0.0102	0.0162	5.0	9147	7526	857
			(b) Local gate error rate of 10^{-4}				
0	0.00217	0.00263	0.00426	1.0	5402	4134	636
1	0.00354	0.000246	0.00369	2.0	6380	5018	695
2	0.000249	0.00041	0.000617	4.1	8369	6818	814
			(c) Local gate error rate of 10^{-5}				
0	0.000214	0.000251	0.000413	1.0	5402	4134	636
1	0.000351	0.000022	0.000364	2.0	6366	5005	694
2	0.0000224	0.0000356	0.0000544	4.0	8296	6751	810

TABLE IX. Simulation results of purification after encoding with postselection for a Bell pair consisting of a single layer of the Steane [[7,1,3]] code and a distance-3 surface code. Raw Bell pairs are created using local gates. Other conditions and definitions are as in Table I. Note that one round of purification at $p = 10^{-5}$ finds only four residual Z errors in 100×10^6 output Bell pairs and that two rounds of purification at $p = 10^{-5}$ find only one residual X error and only two residual Z errors in 100×10^6 output Bell pairs.

No. of purifications	X error rate	Z error rate	Merged error rate	Physical Bell pair inefficiency	KQ	No. of single-qubit gates	No. of two-qubit gates
			(a) Local gate error rate of 10^{-3}				
0	0.0203	0.0251	0.0402	1.0	5402	4134	636
1	0.0303	0.000142	0.0304	2.4	6705	5316	712
2	0.000323	0.000246	0.000556	6.3	10230	8511	917
			(b) Local gate error rate of 10^{-4}				
0	0.0021	0.00261	0.00418	1.0	5402	4134	636
1	0.00301	0.00000141	0.00301	2.0	6395	5033	696
2	0.00000269	0.00000218	0.00000481	4.2	8446	6888	819
			(c) Local gate error rate of 10^{-5}				
0	0.000203	0.000251	0.000405	1.0	5402	4134	636
1	0.000298	0.00000004	0.000298	2.0	6367	5007	694
2	0.00000001	0.00000002	0.00000003	4.0	8304	6758	811

However, architectures that can use this method are more limited in scalability. Thus, this method may be used for standalone code converters, but will not be the preferred method when building scalable quantum internetworking repeaters.

[1] H.-J. Briegel, W. Dür, J. I. Cirac, and P. Zoller, Phys. Rev. Lett. **81**, 5932 (1998).

[2] W. Dür, H.-J. Briegel, J. I. Cirac, and P. Zoller, Phys. Rev. A **59**, 169 (1999).

[3] R. Van Meter, IEEE Network **26**, 59 (2012).

[4] H. J. Kimble, Nature (London) **453**, 1023 (2008).

[5] C. Elliott, A. Colvin, D. Pearson, O. Pikalo, J. Schlafer, and H. Yeh, in *Quantum Information and Computation III*, edited by E. J. Donkor, A. R. Pirich, and H. E. Brandt, SPIE Proc. Vol. 5815 (SPIE, Bellingham, 2005).

[6] M. Peev, C. Pacher, R. Allaume, C. Barreiro, J. Bouda, W. Boxleitner, T. Debuisschert, E. Diamanti, M. Dianati, J. F. Dynes, S. Fasel, S. Fossier, M. Frst, J.-D. Gautier, O. Gay, N. Gisin, P. Grangier, A. Happe, Y. Hasani, M. Hentschel, H. Hübel, G. Humer, T. Länger, M. Legr, R. Lieger, J. Lodewyck, T. Lornser, N. Ltkenhaus, A. Marhold, T. Matyus, O. Maurhart, L. Monat, S. Nauerth, J.-B. Page, A. Poppe, E. Querasser, G. Ribordy, S. Robyr, L. Salvail *et al.*, New J. Phys. **11**, 075001 (2009).

[7] M. Sasaki *et al.*, Opt. Express **19**, 10387 (2011).

[8] M. Ben-Or and A. Hassidim, in *Proceedings of the 37th Annual ACM Symposium on Theory of Computing*, edited by H. N. Gabow and R. Fagin (ACM, New York, 2005), p. 481.

[9] H. Buhrman, R. Cleve, S. Massar, and R. de Wolf, Rev. Mod. Phys. **82**, 665 (2010).

[10] H. Buhrman and H. Röhrig, in *Mathematical Foundations of Computer Science 2003*, edited by B. Rovan and P. Vojtáš, Lecture Notes in Computer Science Vol. 2747 (Springer, Berlin, 2003), p. 1.

[11] H. Buhrman, R. Cleve, and A. Wigderson, *Proceedings of the 30th Annual ACM Symposium on Theory of Computing* (ACM, New York, 1998), p. 63.

[12] C. Monroe, R. Raussendorf, A. Ruthven, K. R. Brown, P. Maunz, L.-M. Duan, and J. Kim, Phys. Rev. A **89**, 022317 (2014).

[13] C.-H. Chien, R. Van Meter, and S.-Y. Kuo, J. Emerg. Technol. Comput. Syst. **12**, 9 (2015).

[14] A. Broadbent, J. Fitzsimons, and E. Kashefi, *Formal Methods for Quantitative Aspects of Programming Languages* (Springer, Berlin, 2010), p. 43.

[15] C. Crep´eau, D. Gottesman, and A. Smith, *Proceedings of the 34th Annual ACM Symposium on Theory of Computing* (ACM, New York, 2002).

[16] R. Jozsa, D. S. Abrams, J. P. Dowling, and C. P. Williams, Phys. Rev. Lett. **85**, 2010 (2000).

[17] P. Kómár, E. Kessler, M. Bishof, L. Jiang, A. S. Sorensen, and M. D. Lukin, Nat. Phys. **10**, 582 (2014).

[18] I. L. Chuang, Phys. Rev. Lett. **85**, 2006 (2000).

[19] S. D. Bartlett, T. Rudolph, and R. W. Spekkens, Rev. Mod. Phys. **79**, 555 (2007).

[20] W. J. Munro, S. J. Devitt, and K. Nemoto, *Proceedings of SPIE Optical Engineering + Applications* (International Society for Optics and Photonics, Bellingham, 2011), p. 816307.

[21] R. Van Meter, *Quantum Networking* (Wiley, New York, 2014).

[22] M. Takeoka, S. Guha, and M. M. Wilde, Nat. Commun. **5**, 5235 (2014).

[23] L.-M. Duan, M. D. Lukin, J. I. Cirac, and P. Zoller, Nature (London) **414**, 413 (2001).

[24] P. van Loock, T. D. Ladd, K. Sanaka, F. Yamaguchi, K. Nemoto, W. J. Munro, and Y. Yamamoto, Phys. Rev. Lett. **96**, 240501 (2006).

[25] N. Sangouard, C. Simon, H. de Riedmatten, and N. Gisin, Rev. Mod. Phys. **83**, 33 (2011).

[26] L. Jiang, J. M. Taylor, N. Khaneja, and M. D. Lukin, Proc. Natl. Acad. Sci. USA **104**, 17291 (2007).

[27] W. Munro, K. Harrison, A. Stephens, S. Devitt, and K. Nemoto, Nat. Photon. **4**, 792 (2010).

[28] L. Jiang, J. M. Taylor, K. Nemoto, W. J. Munro, R. Van Meter, and M. D. Lukin, Phys. Rev. A **79**, 032325 (2009).

[29] A. G. Fowler, D. S. Wang, C. D. Hill, T. D. Ladd, R. Van Meter, and L. C. L. Hollenberg, Phys. Rev. Lett. **104**, 180503 (2010).

[30] Y. Li, S. D. Barrett, T. M. Stace, and S. C. Benjamin, New J. Phys. **15**, 023012 (2013).

[31] E. Knill and R. Laflamme, arXiv:quant-ph/9608012.

[32] W. J. Munro, A. M. Stephens, S. J. Devitt, K. A. Harrison, and K. Nemoto, Nat. Photo. **6**, 777 (2012).

[33] M. Zwerger, W. Dür, and H. J. Briegel, Phys. Rev. A **85**, 062326 (2012).

[34] T. Inagaki, N. Matsuda, O. Tadanaga, M. Asobe, and H. Takesue, Opt. Express **21**, 23241 (2013).

[35] T. Herbst, T. Scheidl, M. Fink, J. Handsteiner, B. Wittmann, R. Ursin, and A. Zeilinger, Proc. Natl. Acad. Sci. USA **112**, 14202 (2015).

[36] G. Vallone, D. Bacco, D. Dequal, S. Gaiarin, V. Luceri, G. Bianco, and P. Villoresi, Phys. Rev. Lett. **115**, 040502 (2015).

[37] S. J. Devitt, A. D. Greentree, A. M. Stephens, and R. Van Meter, arXiv:1410.3224.

[38] J. T. Anderson, G. Duclos-Cianci, and D. Poulin, Phys. Rev. Lett. **113**, 080501 (2014).

[39] C. D. Hill, A. G. Fowler, D. S. Wang, and L. C. L. Hollenberg, Quantum Inf. Comput. **13**, 439 (2013).

[40] A. M. Stephens, Z. W. E. Evans, S. J. Devitt, and L. C. L. Hollenberg, Phys. Rev. A **77**, 062335 (2008).

[41] J. Kim *et al.*, IEEE Photon. Technol. Lett. **15**, 1537 (2003).

[42] M. Ahsan, R. Van Meter, and J. Kim, ACM J. Emerg. Technol. **12**, 39 (2015).

[43] A. J. Landahl, J. T. Anderson, and P. R. Rice, arXiv:1108.5738.

[44] D. Copsey, M. Oskin, F. T. Chong, I. Chuang, and K. Abdel-Ghaffar, First Workshop on Non-Silicon Computing (unpublished).

[45] M. Oskin, F. Chong, and I. Chuang, Computer **35**, 79 (2002).

[46] D. D. Thaker, T. S. Metodi, A. W. Cross, I. L. Chuang, and F. T. Chong, SIGARCH Comput. Archit. News **34**, 378 (2006).

[47] T. S. Metodi, A. I. Faruque, and F. T. Chong, Syn. Lect. Comput. Archit.e **6**, 1 (2011).

[48] B.-S. Choi, *2013 International Conference on ICT Convergence (ICTC)* (IEEE, Piscataway, 2013), p. 1083.

[49] T. Jochym-O'Connor and R. Laflamme, Phys. Rev. Lett. **112**, 010505 (2014).
[50] A. Paetznick and B. W. Reichardt, Phys. Rev. Lett. **111**, 090505 (2013).
[51] B.-S. Choi, Quantum Inf. Process. **14**, 2775 (2015).
[52] A. Steane, Proc. R. Soc. London A **452**, 2551 (1996).
[53] A. M. Steane, Nature (London) **399**, 124 (1999).
[54] S. Buchbinder, C. Huang, and Y. Weinstein, Quantum Inf. Process. **12**, 699 (2013).
[55] E. Dennis, A. Kitaev, A. Landahl, and J. Preskill, J. Math. Phys. **43**, 4452 (2002).
[56] S. Bravyi and A. Kitaev, Phys. Rev. A **71**, 022316 (2005).
[57] M. Kleinmann, H. Kampermann, T. Meyer, and D. Bruß, Phys. Rev. A **73**, 062309 (2006).
[58] W. Dür and H.-J. Briegel, Phys. Rev. Lett. **90**, 067901 (2003).
[59] W. Dür and H. Briegel, Rep. Prog. Phys. **70**, 1381 (2007).
[60] C. Nölleke, A. Neuzner, A. Reiserer, C. Hahn, G. Rempe, and S. Ritter, Phys. Rev. Lett. **110**, 140403 (2013).
[61] J. Kim and C. Kim, Quantum Inf. Comput. **9**, 181 (2009).
[62] R. Van Meter, T. D. Ladd, A. G. Fowler, and Y. Yamamoto, Int. J. Quantum Inf. **8**, 295 (2010).
[63] L. Jiang, J. M. Taylor, A. S. Sørensen, and M. D. Lukin, Phys. Rev. A **76**, 062323 (2007).
[64] D. K. L. Oi, S. J. Devitt, and L. C. L. Hollenberg, Phys. Rev. A **74**, 052313 (2006).